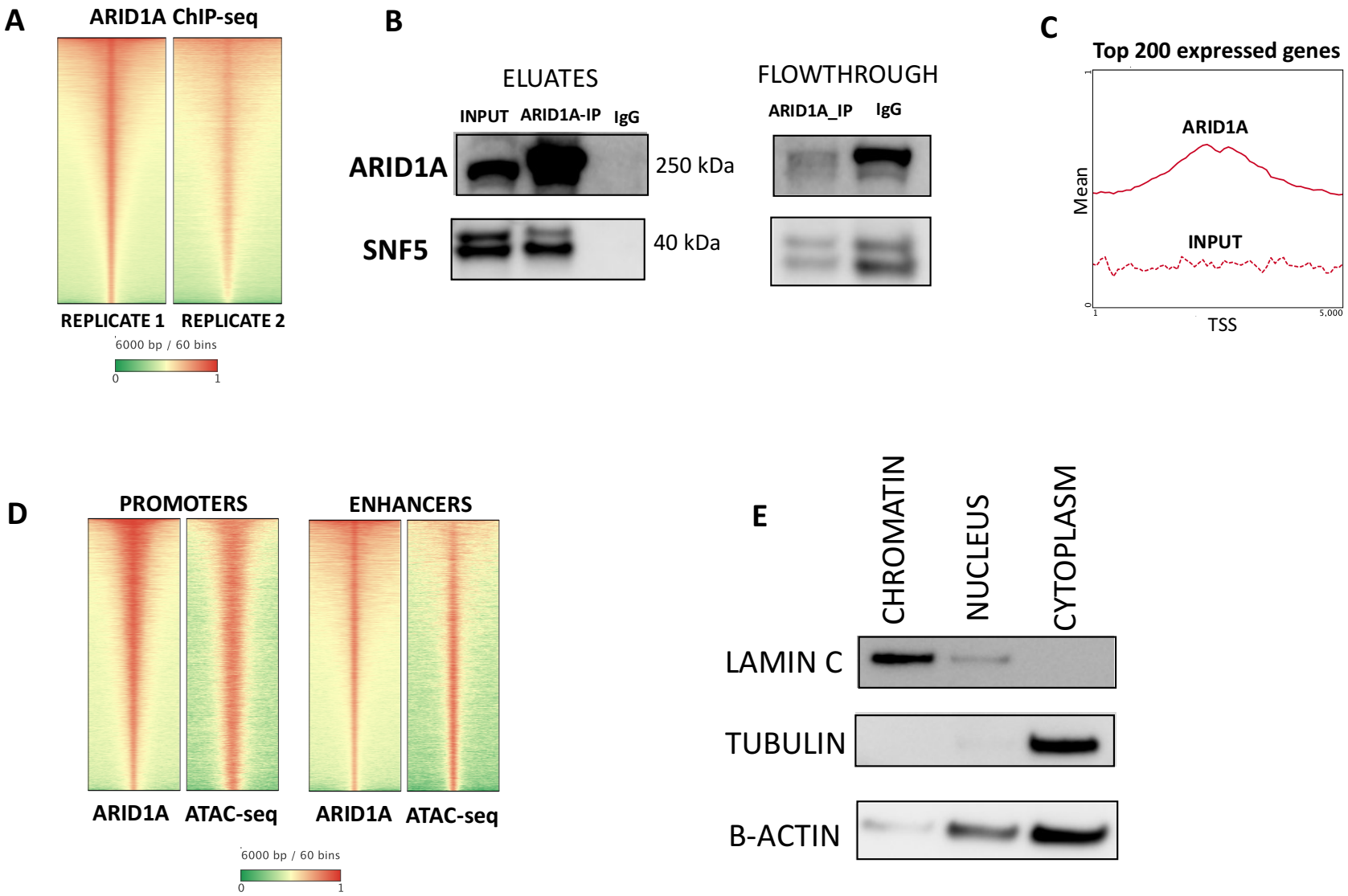

Figure S1, Related to Fig. 1 – ARID1A binds at promoters and enhancers: **(A)** Heatmaps comparing the consistency of of ChIP-seq signal intensity in the two ARID1A replicates (50,951 peaks). **(B)** Immunoprecipitation for ARID1A support ARID1A as member of the SWI/SNF complex and also support the specificity of the antibody used for ChIP-seq. **(C)** Average profile of ARID1A ChIP-seq at the TSSs of the top 200 expressed genes shows strong enrichment for ARID1A compared to input. **(D)** Heatmaps with ARID1A ChIP-seq and ATAC-seq data demonstrate that regions bound by ARID1A are highly accessibly at both enhancers and promoters. **(E)** Control Immunoblots on RMG1 fractionated extracts support the quality of the fractionation.

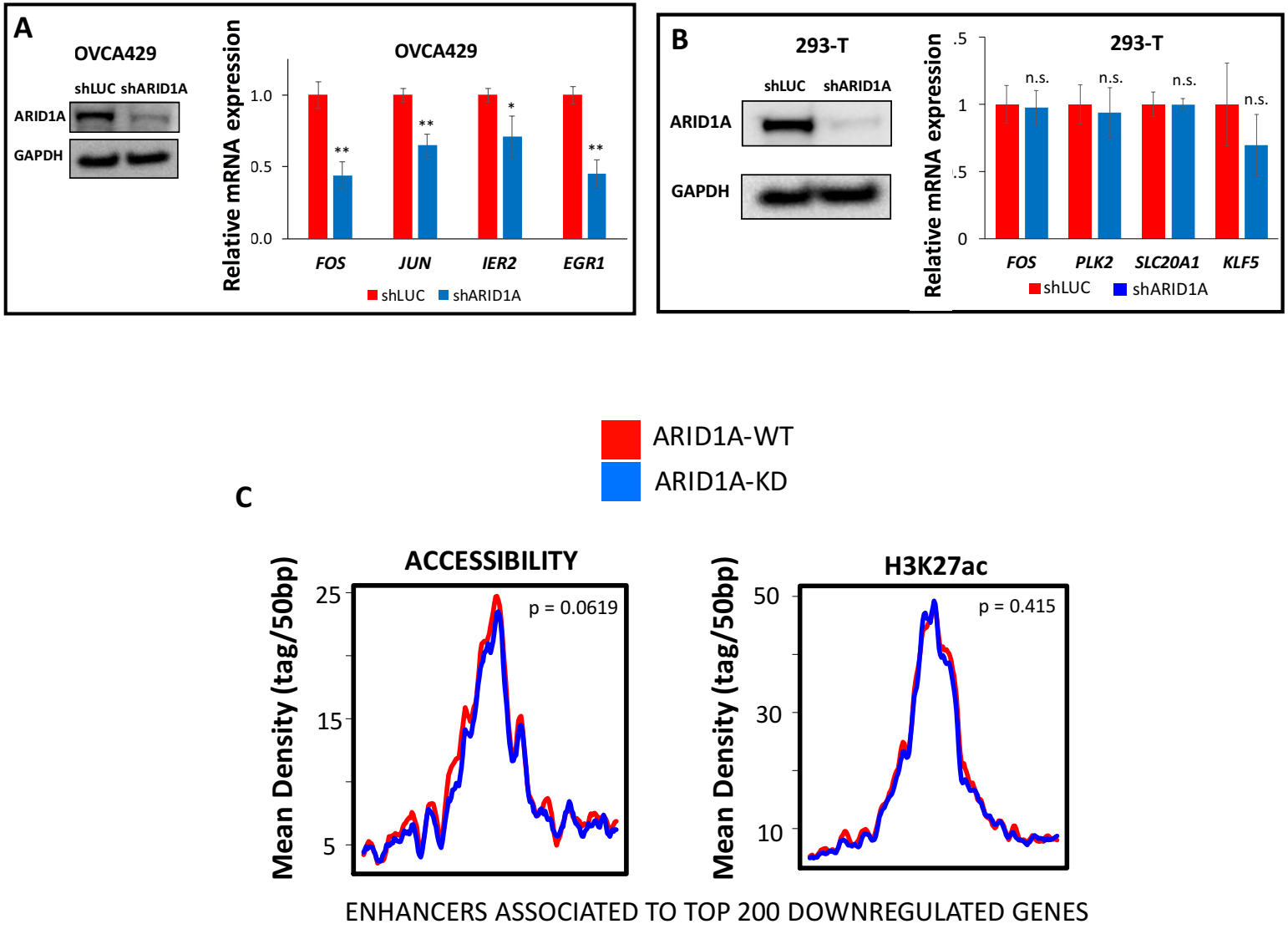

Figure S2, Related to Fig. 2 – (A) qRT-PCR at candidate genes shows that mRNA transcription is significantly diminished upon ARID1-KD in OVCA429 cells (* = p <0.01; ** = p < 0.001) **(B)** qRT-PCR at candidate genes demonstrates that mRNA transcription is not significantly affected by ARID1-KD in 293-T cells. **(C)** ATAC-seq and ChIP-seq for H3K27ac suggest that the enhancers associated to the TOP 200 downregulated genes are not characterized by decrease in either accessibility, nor histone acetylation.

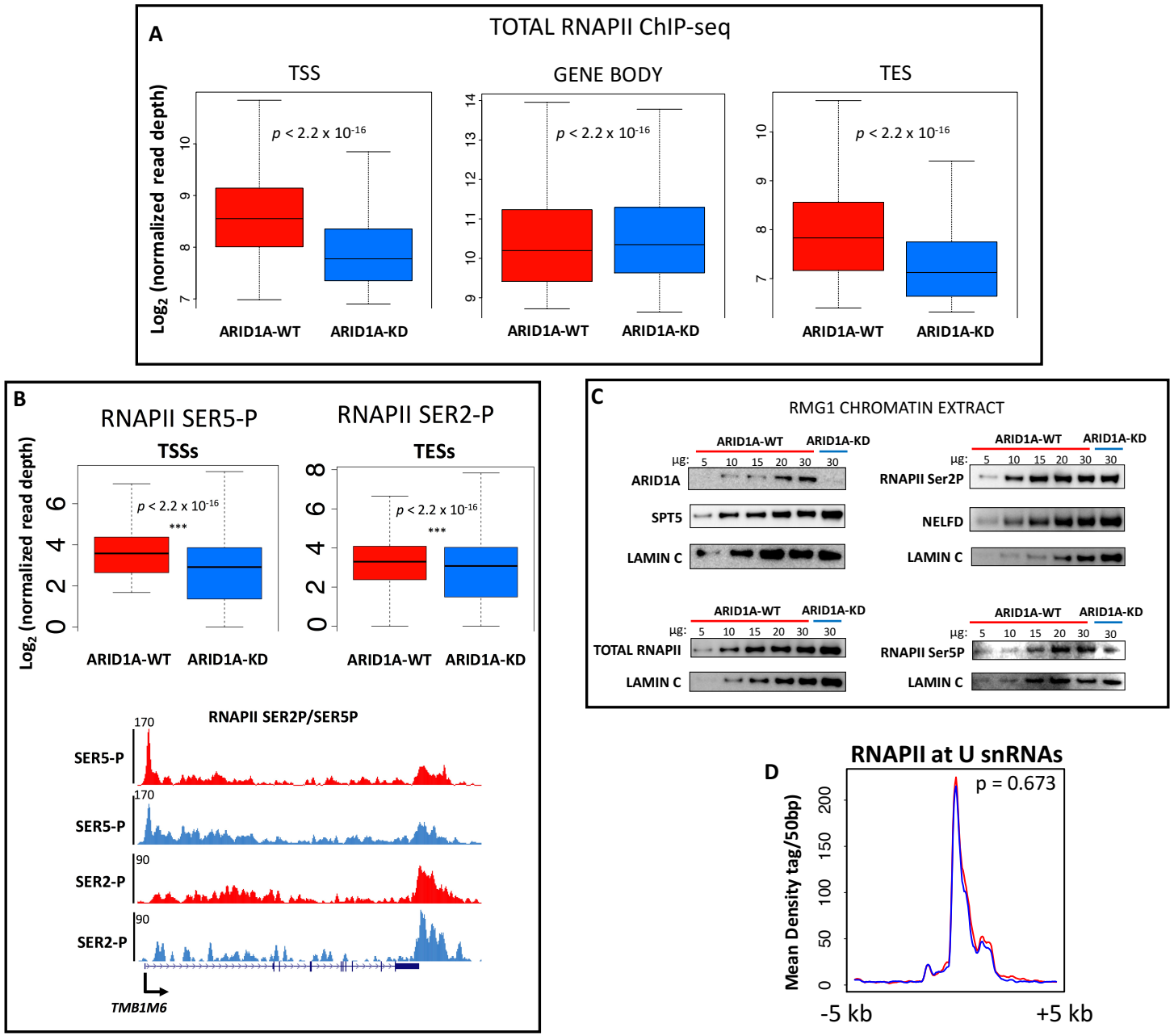

Figure S3, Related to Fig. 4 – (A) Boxplots depict levels of RNAPII occupancy, in ARID1A-WT and ARID1A-KD conditions, at TSS (-50/+300bp), GENE BODY (center point of the the gene body +/-25% of the gene body length), and TES (+/-300bp). Data are normalized by sequencing depth. Loss of RNAPII is limited to TSS and TES regions, while a moderate, but significant, increase of RNAPII is detected on the gene bodies. **(B)** ChIP-seq of Ser2- and Ser5-Phosphorilated RNAPII-CTD supports a strong decrease of Ser5P at the promoter regions, and only a moderate changes of Ser2P at transcription end sites, as exemplified by Genome Browser track for *TMB1M6*. **(C)** Quantitative Western Blots on RMG-1 chromatin extract for ARID1A, Total RNAPII, RNAPII Ser2P, RNAPII Ser5p, NELFD, SPT5. The blots support a >95% KD for ARID1A, and a ca. 40% depletion for RNAPII Ser5P. Levels of the other tested proteins are unchanged upon ARID1A-KD. **(D)** RNAPII levels at U snRNAs are not affected by ARID1A-KD, as suggested by ChIP-seq data.

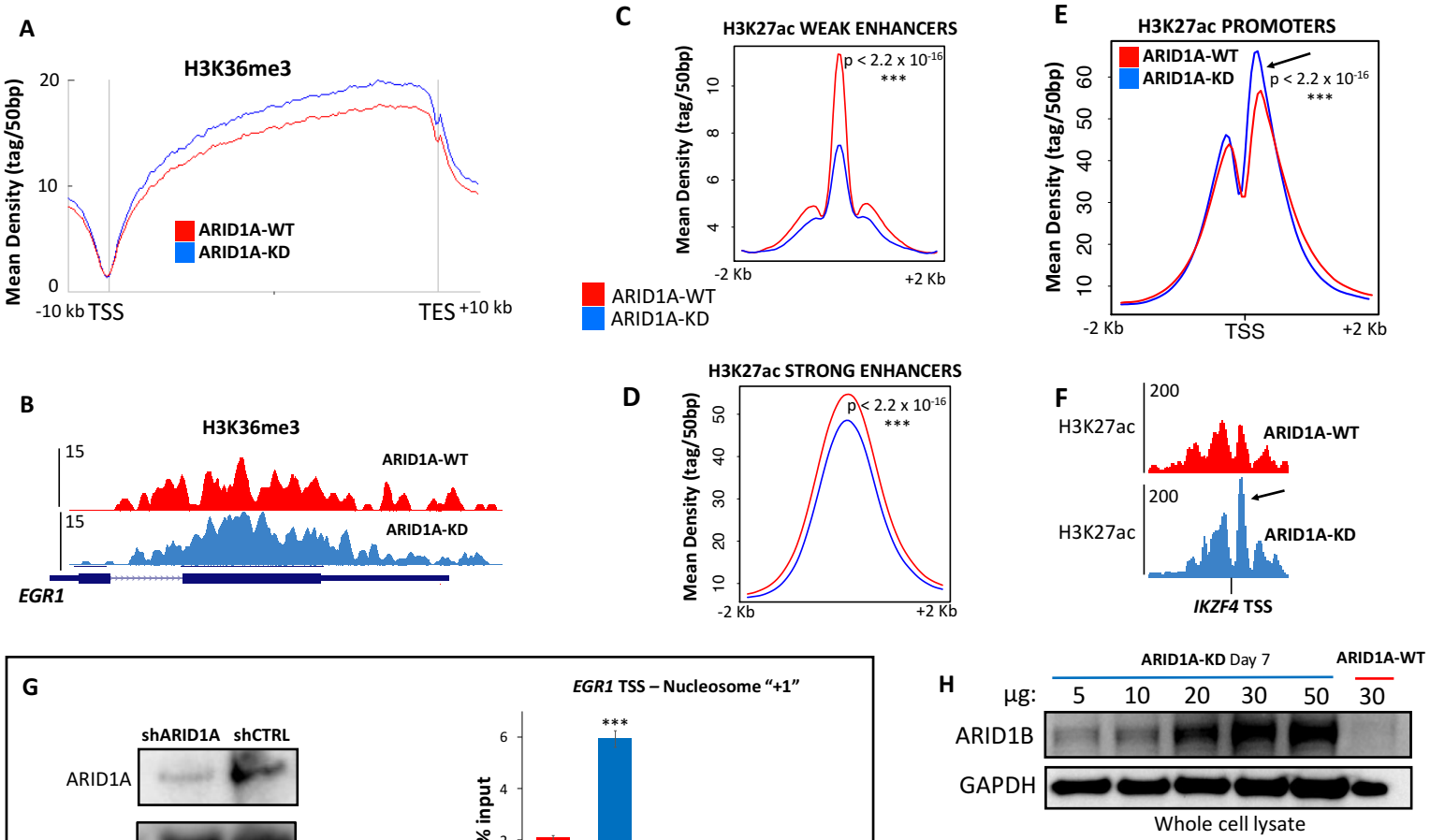

Figure S4, Related to Fig. 5 – (A) Average H3K36me3 ChIP-seq profiles (ARID1A-WT, KD) for all active coding genes reveal a significant increase in H3K36me3 levels upon ARID1A depletion. **(B)** UCSC Genome Browser screenshot depicts H3K36me3 ChIP-seq at the EGR1 locus. **(C)** H3K27ac ChIP-seq average profiles show that H3K27ac levels are severely reduced at weak enhancers upon ARID1A-KD. **(D)** H3K27ac ChIP-seq average profiles show that H3K27ac levels are moderately, but significantly, reduced at strong enhancers. **(E)** Average H3K27ac ChIP-seq profiles at the TSS display a significant increase of acetylation levels at the first nucleosome downstream of the TSS (+1) in ARID1A-KD condition. **(F)** UCSC Genome Browser screenshot showing H3K27ac ChIP-seq at the IKZF4 TSS. **(G)** ChIP-qPCRs at candidate genes show that, upon depletion of ARID1A in RMG-1, levels of H3K27ac at the nucleosome "plus 1" of the transcription start sites increase significantly (*** = $p < 0.0001$). **(H)** Quantitative Western Blot compares ARID1B levels between ARID1A-WT and the day 7 of ARID1A-KD. The blot demonstrates that ARID1B is significantly upregulated as a consequence of ARID1A-KD.

Supplemental Experimental Procedures

Cell lines

RMG-1 cells were obtained from JCRB Cell Bank and maintained in DMEM/F12 50/50 medium (Corning) supplemented with 10% (v/v) of TET-free fetal bovine serum (Clontech) or super calf serum (GEMcell) and 2 mM of L-glutamine (Corning). OVCA429 were obtained from JCRB Cell Bank and maintained in D-MEM medium (Corning) supplemented with 10% (v/v) of super calf serum, 0.1 mM Non-Essential Amino Acids, and 2 mM of L-glutamine.

The RMG1 cell line was infected with lentivirus carrying the inducible tet-pLKO-shARID1A (sequence: GCCTGATCTATCTGGTTCAAT) generated from the tet-pLKO-puro empty vector (Addgene #21915). Single cell clones were selected with 2 µg/ml Puromycin (InvivoGen), isolated and incubated for 72h with 2 µg/ml doxycycline to induce the expression of the shRNA. Medium was changed and doxycycline was provided freshly every 48h. Depletion of ARID1A was detected by Western Blot and clones showing a depletion of the protein higher than 80% were selected.

For validation experiments, ARID1A was depleted using a different shRNA (CCTCTCTTATACACAGCAGAT). For rescue experiments, parental RMG-1 cells were simultaneously infected with a lentivirus carrying the shARID1A vector, and with a lentivirus carrying the pLVX-ARID1A vector. The pLVX empty vector was used as a control. Infected cells were selected with 2 µg/ml Puromycin for 72 hours.

For ARID1B rescue experiments, a commercial plasmid was used (addgene: CMV-T7-hOsa2, ID 17987). The plasmid was transfected in ARID1A-KD RMG-1 cells using

Lipofectamine 2000 (Invitrogen), following manufacturer's protocol. Transfected cells were selected with 2 µg/ml Puromycin for 72 hours.

OVCA429 cells were lentivirally infected with pLKO.1-shARID1A (TRCN0000059090), obtained from the Molecular Screening Facility at the Wistar Institute, and selected with 2 µg/ml Puromycin. A shRNA against luciferase was used as control.

Western Blot

For total lysate, cells were harvested and washed three times in 1X PBS and lysed in RIPA buffer (50 mM Tris-HCl pH 7.5, 150 mM NaCl, 1% Igepal, 0.5% sodium deoxycholate, 0.1% SDS, 500 uM DTT) with proteases inhibitors. 50 µg of whole cell lysate were loaded in Bolt 4-12% Bis-Tris Plus gel (Invitrogen) and separated through gel electrophoresis (SDS-PAGE) in Bolt MES running buffer (Invitrogen). Separated proteins were then transferred to ImmunBlot PVDF membranes (BioRad) for antibody probing. Membranes were incubated with 10% BSA in TBST for 30 minutes at room temperature (RT), then incubated for variable times with the suitable antibodies diluted in 5% BSA in 1X TBST, washed with TBST and incubated with a dilution of 1:10000 of secondary antibody for one hour at RT. The antibody was then visualized using Clarity Western ECL substrate (Biorad) and imaged with Fujifilm LAS-3000 Imager.

For quantitative western blots, RMG-1 chromatin extract was isolated, and to quantify the depletions, different amounts of ARID1A-WT chromatin extracts were loaded, with a gradient ranging from 5 to 30 ug.

Antibodies

ARID1A ChIP-seq: Abcam ab97995 (replicate 1), ab182560 (replicate 2). ARID1A western blot: Cell Signaling Technology #12354. ARID1B western blot, ChIP-qPCR: ABGENT AT1189a. H3K27ac ChIP-seq: Abcam ab4279. H3K36me3 ChIP-seq: Abcam ab9050. Total RNAPII western blot: mouse Santa Cruz A10 (SC-17798); custom rabbit polyclonal antibody raised against the N-terminal domain. Serine-5P RNAPII-CTD western blot: Santa Cruz CTD-4H8 (SC-47701). Serine-5P RNAPII-CTD ChIP-seq: Active Motifs 3E8 (61086). Total RNAPII ChIP-seq: custom rabbit polyclonal antibody raised against the N-terminal domain. Serine-2P RNAPII-CTD western blot and ChIP-seq: Active Motifs 3E10 (61084). GAPDH western blot: Cell Signaling 14C10. LAMIN A/C western blot: Santa Cruz 346 sc-7293. NELFD western blot: Santa Cruz C10 (sc-393972). SPT5 western blot: Santa Cruz D-3 (sc-133217). Cell Signaling HRP-conjugated goat anti-rabbit (7074S) and horse anti-mouse (7076S) were used as secondary antibodies in western blot. Beta-Actin: anti-actin-HRP (Sigma). Tubulin: (Sigma, 79026).

ChIP-seq and ChIP-qPCR sample processing

Samples from different conditions were processed together to prevent batch effects. For each replicate, 10 million RMG-1 cells were cross-linked with 1% formaldehyde for 5 min at room temperature, harvested and washed twice with 1× PBS. The pellet was resuspended in ChIP lysis buffer (150 mM NaCl, 1% Triton-X 100, 0,7% SDS, 500 µM DTT, 10 mM Tris-HCl, 5 mM EDTA) and chromatin was sheared to an average length of 200–400 bp, using a Covaris S220 Ultrasonicator. The chromatin lysate was diluted with SDS-free ChIP lysis buffer. For ChIP-seq, 10 µg of antibody (5 µg for histone

modifications) was added to the 10 million lysated cells along with Protein A magnetic beads (Invitrogen) and incubated at 4 °C overnight. On day 2, beads were washed twice with each of the following buffers: Mixed Micelle Buffer (150 mM NaCl, 1% Triton-X 100, 0.2% SDS, 20 mM Tris-HCl, 5 mM EDTA, 65% sucrose), Buffer 500 (500 mM NaCl, 1% Triton-X 100, 0.1% Na deoxycholate, 25 mM HEPES, 10 mM Tris-HCl, 1 mM EDTA), LiCl/detergent wash (250 mM LiCl, 0.5% Na deoxycholate, 0.5% NP-40, 10 mM Tris-HCl, 1 mM EDTA) and a final wash was performed with 1× TE. Finally, beads were resuspended in 1× TE containing 1% SDS and incubated at 65 °C for 10 min to elute immunocomplexes. Elution was repeated twice, and the samples were further incubated overnight at 65 °C to reverse cross-linking, along with the untreated input (5% of the starting material). On day 3, after treatment with 0.5 mg/ml proteinase K for 3 h, DNA was purified with Zymo ChIP DNA Clear Concentrator kit and quantified with QUBIT.

Barcoded libraries were made with NEB ULTRA II DNA Library Prep Kit for Illumina, and sequenced on Illumina NextSeq 500, producing 75bp SE reads.

For ChIP-qPCR, on day 1 the sonicated lysate was aliquoted into single immunoprecipitations of 2.5 × 10^6 cells each. A specific antibody or a total rabbit IgG control was added to the lysate along with Protein A magnetic beads (Invitrogen) and incubated at 4 °C overnight. On day3, ChIP eluates and input were assayed by real-time quantitative PCR in a 20 µl reaction with the following: 0.4 µM of each primer, 10 µl of iQ SYBR Green Supermix (BioRAD), and 5 µl of template DNA (corresponding to 1/40 of the elution material) using a CFX96 real-time system (BioRAD). Thermal cycling parameters were: 3 min at 95 °C, followed by 40 cycles of 10 s at 95 °C, 20 s at 63 °C followed by 30 s at 72 °C.

For flavopiridol experiments, ARID1A-WT and ARID1A-KD cells were treated with flavopiridol (2μM) for two hours before being harvested.

ChIP-seq analyses

Sequences were aligned to the reference hg19, using Burrows Wheeler Alignment tool (BWA), with the MEM algorithm (Li, 2013). Aligned reads were filtered based on mapping quality (MAPQ > 10) to restrict our analysis to higher quality and likely uniquely mapped reads, and PCR duplicates were removed. We called peaks for each individual using MACS2, at 5% FDR, with default parameters (Zhang et al., 2008). Heatmaps were generated with ChAsE v. 1.0.11 (Younesy et al., 2016), average profiles with seqMINER (Ye et al., 2011). Read density based average profiles were generated using seqMINER v. 1.3.4 (Zhan and Liu, 2015)

RNAPII travelling curve was produced computing the ratio between read depth at the TSS (-50/+500 bp) and the rest of the genes, for all of the genes with an overlapping RNAPII peak at the TSS in both conditions.

Classification of weak and strong enhancers

Quartile distribution analysis was performed on H3K27ac normalized read depth at enhancers for ARID1A-WT cells. Enhancers included in first and second quartile were defined as *weak.* Enhancers included in third and fourth quartile were defined as *strong.*

ATAC-seq sample processing

Two independent biological replicates of 50,000 cells per condition were processed literally as described in the original ATAC-seq protocol paper (Buenrostro et al., 2013). Barcoded samples were sequenced on Illumina NextSeq 500, producing 75bp SE reads.

ATAC-seq analyses

ATAC-seq data were processed with the same pipeline described for ChIP-seq, with one modification: all mapped reads were offset by +4 bp for the forward-strand and -5 bp for the reverse-strand. After peak calling, peaks replicated in both of the two ARID1A-WT samples (hereafter consensus peaks) were used for downstream analyses. Specifically, we used BEDtools v2.25.0 (Quinlan and Hall, 2010) to map read coverage on the set of consensus peaks for each sample in both conditions. EdgeR (Robinson et al., 2010) was used to test for regions with differential accessibility between ARID1A-KD and ARID1A-WT, using a likelihood ratio test in a generalized linear model with the following parameters: glmLRT(fit,coef=2), based on quantile-normalized read counts.
Read density based average profiles were generated using seqMINER v. 1.3.4 (Zhan and Liu, 2015).

RNA-seq sample processing

Total RNA-seq was performed on two independent biological replicates per condition. Samples from different conditions were processed together to prevent batch effects. For each sample, 10 million cells were used to extract total RNA using Zymo Direct-Zol RNA miniprep Kit. 50,000 S2 Drosophila cells were used as spike in control for the RNA-seq experiments. Quality of total RNA was assessed by the RNA Integrity Number (RIN) using

Agilent Bioanalyzer. All retained RNA samples had a RIN > 8.

1 µg of total or chromatin-bound RNA were depleted of ribosomal RNA using the NEBNext rRNA depletion kit (New England Biolabs). rRNA-depleted RNA was purified with the miRNEasy kit (Qiagen) and used to produce barcoded RNA sequencing libraries using the NEBNext Ultra Directional RNA Library Prep kit, and sequenced on Illumina NextSeq 500, producing 75bp SE reads.

RNA-seq analyses

Reads were aligned to hg19 using STAR v2.5 (Dobin et al., 2013), in 2-pass mode with the following parameters: --quantMode TranscriptomeSAM --outFilterMultimapNmax 10 --outFilterMismatchNmax 10 --outFilterMismatchNoverLmax 0.3 --alignIntronMin 21 --alignIntronMax 0 --alignMatesGapMax 0 --alignSJoverhangMin 5 --runThreadN 12 --twopassMode Basic --twopass1readsN 60000000 --sjdbOverhang 100. We filtered bam files based on alignment quality (q = 10) using Samtools v0.1.19 (Li et al., 2009). We used the latest annotations obtained from Ensembl to build reference indexes for the STAR alignment. FeatureCounts (Liao et al., 2014) was used to count reads mapping to each gene. RSEM (Li and Dewey, 2011) was instead used to obtain FPKM (Fragments Per Kilobase of exon per Million fragments mapped). We analyzed differential gene expression levels with DESeq2 (Love et al., 2014), with the following model: design = ~condition, where condition indicates either ARID1A-WT or ARID1A-KD.

GRO-seq

GRO-seq was performed on two independent biological replicates per condition as previously described (Gardini et al., 2014). Briefly, cells were washed twice with ice-cold PBS before adding swelling buffer. Cells were swelled for 5 min on ice and then lysed in lysis buffer. Nuclei were washed twice with lysis buffer and resuspended in 100 µl freezing buffer. An equal volume of reaction buffer was added and incubated for 7 min at 30°C for the nuclear run-on. Nuclear run-on RNA was extracted with TRIzol LS reagent (Invitrogen) following the manufacturer's instructions and ethanol precipitated. Resuspended NRO-RNA was treated with DNase (Ambion) for 30 min and hydrolyzed using fragmentation reagents (Ambion) for 13 min at 70°C. After purification through a Micro Bio-Spin p-30 column (Bio-Rad), T4 PNK (NEB) was used to repair the NRO-RNA ends. The Br-UTP-labeled NRO-RNA was then purified by anti-BrdU agarose beads (Santa Cruz Biotechnology) in binding buffer for 1 hr. Following elution, RNA was ethanol precipitated prior to denaturing RNA and treating with poly(A)-polymerase (NEB) for 30 min at 37°C. cDNA synthesis was performed using oNTI223 primer. The reaction was treated with 3 µl exonuclease I (Fermentas) for 15 min at 37°C, followed by 2 µl 1M NaOH for 20 min at 98°C, and neutralized with 1 µl 2M HCl. cDNA was run on a 10% TBE-urea gel, and products were excised and eluted from shredded gel pieces for 4 hr in TE + 0.1% Tween and precipitated in ethanol overnight. First-strand cDNA was circularized with CircLigase (Epicenter), denatured for 10 min at 80°C, and relinearized with APE I (NEB). Linearized DNA was amplified by PCR using the Phusion Hot Start II Kit, according to manufacturer's instructions. The oligonucleotide primers oNTI200 and oNTI201 were used for amplification. The PCR product was run on a 10% TBE gel and eluted as before. Libraries were sequenced on an NextSeq 500 producing 75bp SE reads.

GRO-seq data were analyzed with the same pipeline above described for total RNA-seq. The annotations for the 1,550 ribosomal genes showed in Fig. 3 were obtained from "rRNA transcript type" annotation file in v17 of GENCODE.

Statistical and genomic analyses

All statistical analyses were performed using R v3.3.1. Figures were made with the package ggplot2 (Wickham, 2009). BEDtools v2.27.1 was used for genomic analyses. For travelling ratio analysis, TSS regions were extended -50/+300bp. Other thresholds were tested (up to +500 bp downstream), with no differences in the results. Pathway analysis was performed with Ingenuity Pathway Analysis Suite (QIAGEN Inc., https://www.qiagenbioinformatics.com/products/ingenuity-pathway-analysis). Motif analyses were performed using the Meme-Suite (Bailey et al., 2009), and specifically with the Meme-ChIP application. Fasta files of the regions of interest were produced using BEDTools v2.27.1. Shuffled input sequences were used as background. E-values < 0.001 were used as threshold for significance (Bailey et al., 2009).

LIST OF PRIMERS USED FOR THE STUDY			
PRIMER NAME	**SEQUENCE**	**TARGET**	**APPLICATION**
18S-1f	ATACATGCCGACGGGCGCTG	18s rRNA	qRT-PCR
18S-1r	AGGGGCTGACCGGGTTGGTT	18s rRNA	qRT-PCR
Ad1	AATGATACGGCGACCACCGAGATCTACACTCGTCGGCAGCGTCAGATGTG	LIBRARIES	ATACSEQ
Ad2.2	CAAGCAGAAGACGGCATACGAGATCTAGTACGGTCTCGTGGGCTCGGAGATGT	LIBRARIES	ATACSEQ
Ad2.5	CAAGCAGAAGACGGCATACGAGATAGGAGTCCGTCTCGTGGGCTCGGAGATGT	LIBRARIES	ATACSEQ
EGR1_fw	AGCCCTACGAGCACCTGAC	EGR1 mRNA	qRT-PCR
EGR1_rv	GGTTTGGCTGGGGTAACTG	EGR1 mRNA	qRT-PCR
EGR1_TSS_CHIP_F	CTGATGTCCCCGCTGCAGAT	EGR1 TSS	ChIP-qPCR
EGR1_TSS_CHIP_R	GGTAGTTGTCCATGGTGGGC	EGR1 TSS	ChIP-qPCR
FOS-F	CCAAGACTGAGCCGGCGGCC	FOS TSS	ChIP-qPCR

FOS-R	ACAGGTGGGCGCTGTGGAGC	FOS TSS	ChIP-qPCR
IER2 (1) fw	GAAAACCGTGGAGAGAAGCC	IER2 TSS	ChIP-qPCR
IER2 (1) rv	GTTCACGTCCCAGTCCACTA	IER2 TSS	ChIP-qPCR
IER2 (2) fw	TGACGTCACTGAGACACCCC	IER2 mRNA	qRT-PCR
IER2 (2) rv	CGCAACTTCAGTTTCCCTTC	IER2 mRNA	qRT-PCR
JUN-For	GCCCAGAGCTAGCGCCTGTG	JUN TSS and mRNA	qRT-PCR
JUN-Rev	CTGTCAACAGCGCCTGGGCA	JUN TSS and mRNA	qRT-PCR
JUND_TSS_F	TGTGCGCCCTCTTATAGCCT	JUND TSS and mRNA	qRT-PCR
JUND_TSS_R	CCTCCATGCAAATGAGCGACG	JUND TSS and mRNA	qRT-PCR
KLF5_RT_V2_F	GCAATCCCAGTCTCTCCAAA	KLF5 mRNA	qRT-PCR
KLF5_RT_V2_R	ACTTTTTATGCTCTGGAATTATAGGAA	KLF5 mRNA	qRT-PCR
KLF5_TSS_F	GGGCGTCAAGTGTCAGTAGTC	KLF5 TSS	ChIP-qPCR
KLF5_TSS_R	ACCGTGCTCTCAGGCTCTC	KLF5 TSS	ChIP-qPCR
NTI200-5	CAAGCAGAAGACGGCATACGAGATCACTGTGTGACTGGAGTTCAGACGTGTGCTCTTCCGATC	LIBRARIES	GROSEQ
NTI200-6	CAAGCAGAAGACGGCATACGAGATATTGGCGTGACTGGAGTTCAGACGTGTGCTCTTCCGATC	LIBRARIES	GROSEQ
NTI200-7	CAAGCAGAAGACGGCATACGAGATGATCTGGTGACTGGAGTTCAGACGTGTGCTCTTCCGATC	LIBRARIES	GROSEQ
PLK2_RT_F	TTGGCTGCGTAACTGTGAAC	PLK2 mRNA	qRT-PCR
PLK2_RT_R	ACTGCTCTTTGGGCTGTAATAAA	PLK2 mRNA	qRT-PCR
PLK2_TSS_F	GTGGTCCTCGCACCCTTG	PLK2 TSS	ChIP-qPCR
PLK2_TSS_R	AGCGCTCTCACTCGCACA	PLK2 TSS	ChIP-qPCR
SLC20A1_RT_F	GGCCTTCCCATCAGTACAAC	SLC20A1 mRNA	qRT-PCR
SLC20A1_RT_R	AAGAGACGCCAGTCAACAGC	SLC20A1 mRNA	qRT-PCR

Supplemental References

Bailey, T.L., Boden, M., Buske, F.A., Frith, M., Grant, C.E., Clementi, L., Ren, J., Li, W.W., and Noble, W.S. (2009). MEME SUITE: tools for motif discovery and searching. Nucleic Acids Res *37*, W202-208.

Buenrostro, J.D., Giresi, P.G., Zaba, L.C., Chang, H.Y., and Greenleaf, W.J. (2013). Transposition of native chromatin for fast and sensitive epigenomic profiling of open chromatin, DNA-binding proteins and nucleosome position. Nat Methods *10*, 1213-1218.

Dobin, A., Davis, C.A., Schlesinger, F., Drenkow, J., Zaleski, C., Jha, S., Batut, P., Chaisson, M., and Gingeras, T.R. (2013). STAR: ultrafast universal RNA-seq aligner. Bioinformatics *29*, 15-21.

Gardini, A., Baillat, D., Cesaroni, M., Hu, D., Marinis, J.M., Wagner, E.J., Lazar, M.A., Shilatifard, A., and Shiekhattar, R. (2014). Integrator regulates transcriptional initiation and pause release following activation. Mol Cell *56*, 128-139.

Li, B., and Dewey, C.N. (2011). RSEM: accurate transcript quantification from RNA-Seq data with or without a reference genome. BMC Bioinformatics *12*, 323.

Li, H. (2013). Aligning sequence reads, clone sequences and assembly contigs with BWA-MEM.

Li, H., Handsaker, B., Wysoker, A., Fennell, T., Ruan, J., Homer, N., Marth, G., Abecasis, G., Durbin, R., and Genome Project Data Processing, S. (2009). The Sequence Alignment/Map format and SAMtools. Bioinformatics *25*, 2078-2079.

Liao, Y., Smyth, G.K., and Shi, W. (2014). featureCounts: an efficient general purpose program for assigning sequence reads to genomic features. Bioinformatics *30*, 923-930.

Love, M.I., Huber, W., and Anders, S. (2014). Moderated estimation of fold change and dispersion for RNA-seq data with DESeq2. Genome Biol *15*, 550.

Robinson, M.D., McCarthy, D.J., and Smyth, G.K. (2010). edgeR: a Bioconductor package for differential expression analysis of digital gene expression data. Bioinformatics *26*, 139-140.

Quinlan A.R., Hall I.M. (2010). BEDTools: a flexible suite of utilities for comparing genomic features. Bioinformatics *26*, 841-842.

Wickham, H. (2009). ggplot2: Elegant Graphics for Data Analysis. Springer-Verlag New York.

Younesy, H., Nielsen, C.B., Lorincz, M.C., Jones, S.J., Karimi, M.M., and Moller, T. (2016). ChAsE: chromatin analysis and exploration tool. Bioinformatics *32*, 3324-3326.

Zhan, X., and Liu, D.J. (2015). SEQMINER: An R-Package to Facilitate the Functional Interpretation of Sequence-Based Associations. Genet Epidemiol *39*, 619-623.

Zhang, Y., Liu, T., Meyer, C.A., Eeckhoute, J., Johnson, D.S., Bernstein, B.E., Nusbaum, C., Myers, R.M., Brown, M., Li, W.*, et al.* (2008). Model-based analysis of ChIP-Seq (MACS). Genome Biol *9*, R137.